

On the Anomalous Balmer Line Strengths in Globular Clusters

Violet Poole, Guy Worthey, Hyun-chul Lee and Jedidiah Serven

Department of Physics and Astronomy, Washington State University, Pullman, WA 99163

gworthey@wsu.edu

ABSTRACT

Spectral feature index diagrams with integrated globular clusters and simple stellar population models often show that some clusters have weak $H\beta$, so weak that even the oldest models cannot match the observed feature depths. In this work, we rule out the possibility that abundance mixture effects are responsible for the weak indices unless such changes operate to cool the entire isochrone. We discuss this result in the context of other explanations, including horizontal branch morphology, blue straggler populations, and nebular or stellar emission fill-in.

Subject headings: blue stragglers — stars: horizontal-branch — globular clusters: general — stars: abundances — stars: flare

1. Introduction

Globular cluster are often the only objects that can be detected in the halos of other galaxies. Since most globular cluster are very old, studying them provides vital information about the formation and chemical history of these galaxies (Gratton et al. 2004). The similar ages of the constituent stars and low velocity dispersion makes these objects relatively easy to study, in integrated light.

The most reliable way to obtain information about age and abundance patterns of a stellar population is star by star analysis via a color-magnitude diagram (CMD). However this technique is only feasible for nearby objects, due to the limits of current instrumentation. Therefore, we need to develop reliable methods for analyzing the composite light from all the stars in these systems. This is no easy feat, since many factors can complicate the analysis.

One of the biggest problems that plagues the study of the integrated light of a stellar population is the very similar effects that age and metallicity have on the spectra of stellar populations (O’Connell 1986). However, the degeneracy between the age and metallicity can be broken. Rabin (1980, 1982) and Gunn et al. (1981) noticed that the Balmer lines are quite sensitive to age. Combining this with the knowledge that metal lines, such as Mg b , [MgFe], or $\langle\text{Fe}\rangle$, are relatively more sensitive to metallicity than age (Worthey 1994), the degeneracy between age and metallicity can be broken by plotting the strength of the Balmer lines versus metallic absorption blends. This is because $H\beta$ operates in such a way that its strength is nonlinear with temperature, especially between 6000 K and 9000 K, where main-sequence turnoff stars from a few hundred Myr to ancient reside. But stars of other kinds also inhabit that temperature band.

The $H\beta$ -metal-index grids give the impression that age and metallicity are the only factors that affect a population’s location in the grid, but of course this is misleading. As you can see from Fig 1, other factors must be affecting the values of the indices, since they are quite scattered and some are off the grid. For comparison, an average of the Virgo elliptical galactic nuclei is also plotted along with the globular cluster data (J. Serven et al. 2009, in preparation).

Observational difficulties play a mind role, of course. There are sometimes horizontal branch and blue straggler stars that can contribute enough to alter the lines strengths. Rarer stars such as AGB-Manque stars (Greggio & Renzini 1990) and planetary nebula can be ruled out as being significant contributors under ordinary circumstances, as can the much fainter white dwarf population. These warm stars make the Balmer indices stronger, not weaker, so for populations of these stars to represent a “solution” to the mystery, there would also need to be a systematic error in the models to weaker Balmer index strength.

Additionally, there is the possibility that $H\beta$ is being filled in by nebular emission from hydrogen recombination lines. This fill-in could come from diffuse gas, but it could also come from flaring stars of various sorts: asymptotic giant branch (AGB) stars, M-type dwarfs, cataclysmic variables, and others are known to have transient emission-line spectra (Schiavon et al. 2005).

Finally, there is the possibility that abundance-mixture effects could drive a significant change in $H\beta$ and other feature strengths. This is a relatively unexplored avenue of investigation, but the tools now exist to probe the question (Dotter et al. 2007; Lee et al. 2009), and that is our primary task in this paper.

The models and observational data are already available in the literature, but the implementation is recapped in §2. The implications of our investigation are discussed in §3,

and then there is a brief conclusion.

2. Observations and Models

A version of the Trager et al. (1998) models that use synthetic spectra (Lee et al. 2009) was used to create synthetic spectra at a variety of ages and metallicities. The underlying isochrones for this exercise were Worthey (1994), because they would allow us HB morphology control. However, there are certain caveats to using these isochrones. Specifically the models are a bit crude by today’s standards and the ages are about 2 Gyr too old, so that 17 Gyr should really be interpreted as 15 Gyr.

For this exercise, new stellar index fitting functions were generated. The data sources include a variant of the original Lick collection of stellar spectra (Worthey et al. 1994) in which the wavelength scale of each observation has been refined via cross-correlation, as well as the MILES spectral library (Sanchez-Blazquez et al. 2007) with some zero point corrections, and the Coude Feed library (CFL) of Valdes et al. (2004). The CFL was used as the fiducial set, in the sense that any zero point shifts between libraries were corrected to agree with the CFL case. The MILES and CFL spectra were smoothed to a common Gaussian smoothing corresponding to 200 km s⁻¹. The rectified-Lick spectra were measured and then a linear transformation was applied to put it on the fiducial system.

Multivariate polynomial fitting was done in five overlapping temperature swaths as a function of $\theta_{eff} = 5040/T_{eff}$, $\log g$, and [Fe/H]. The fits were combined into a lookup table for final use. As in Worthey (1994), an index was looked up for each “star” in the isochrone and decomposed into “index” and “continuum” fluxes, which added, then re-formed into an index representing the final, integrated value after the summation.

We also smoothed the Schiavon et al. (2005) globular cluster spectra to 200 km s⁻¹ or the Lick (Worthey & Ottaviani 1997) resolution, as needed, and measured Lick or Lick-like pseudo-equivalent width indices (Worthey et al. 1994; Worthey & Ottaviani 1997; Serven et al. 2005) from them. When the globular clusters and the age-metallicity model grid of values were plotted on the same graph (see Figures 2 through 6) a globular cluster’s position in the grid allows one to estimate its age and metallicity, at least naively.

Cursory examination of these graphs yields a puzzling thing. On graphs with H β as one of the indices, some of the globular clusters lie much below the oldest age plotted of 17 Gyr (see Figure 2). However, graphs that are not plotted with the H β index as one of the axes do not have this problem (see Figures 3 through 6). This indicates that there could be something going on in the spectra of these globular clusters near the H β line that does not

affect $H\gamma$ or $H\delta$ to the same degree. It could also indicate that the models for the $H\beta$ index are not correct.

3. Discussion: Balmer Features in the Integrated Light of Globular Clusters

Many factors could potentially affect the Balmer features in the integrated light of the globular clusters. We consider effects due to abundance ratios, horizontal branch morphology, the presence of blue stragglers, and emission fill-in of the Balmer lines due to hydrogen recombination lines from either external nebulae or stellar activity in individual cluster stars. We also consider the illusions due to miscalibrated models.

3.1. Abundance Ratio Effects

It is of interest to examine the spectra themselves for evidence to support the various hypotheses that could explain their behavior. Comparison of the spectra of the globular clusters with ages off the grid to the spectra of globular clusters with similar metallicity lying within the grid indicates that the main difference is the depth of the $H\beta$ line itself, rather than a difference in heights of either the blue or red continuum bands (see Figure 7). Specifically, the $H\beta$ line of the clusters off the grid are shallower and than those that are on the grid, and, morphologically, this does not seem to be a problem in the continuum regions at all, but a true modulation of the $H\beta$ line itself.

Figure 7 should be compared to Figure 8, which shows several model population spectra with $[X/Fe]=0.3$ dex, where X stand for Fe, Mg, Ti, or Ni. Other elements were explored, but these four had the largest impact on the spectrum shape. We note that none of the elements effect the model depth of the $H\beta$ line itself; only modest effects in the continuum regions. Visually, Fe enhancement raises the average height of the red continuum band. Quantitatively, however, this “extra slope” does little to change the actual index value. Furthermore, in comparing model spectra with the observed globular cluster spectra, raising the red continuum flux does not improve the appearance of the spectral match.

A more quantitative way to analyze the effect due to element enhancement is by looking at the spectral response of the indices when the various elements are enhanced in the same way as Serven et al. (2005). The results of these calculations on our model spectra can be found in Table 1. Row 1 is the model index while row 2 is the uncertainty assuming a $S/N = 100$ at 5000 Å. Rows 3 through 25 list the change of index when the labeled element is enhanced by 0.3 dex, while the last row has all elements up by 0.3 dex. As you can see,

most elements, with the exception of iron and possibly nickel, have little to no effect on the $H\beta$ index. This is in agreement, except for Ni, with the observations made directly from the model spectra.

These analyses indicate that the reason for larger spread in ages for grid with the $H\beta$ index as one of the axes, is most likely not due to enhancement of a certain element. However, there is one possible caveat. If abundance ratios make the isochrones cooler and if metal rich globular clusters have a different mix than elliptical galaxies, then it may work out alright. Since we have successfully ruled out abundance ratio effects we can go on to examine other possible reasons.

3.2. Horizontal Branch Morphology

Horizontal branch morphology, that is “red clump,” “extended,” “blue,” or “extreme,” is easy to determine with a good color magnitude diagram of the stars within the globular cluster, but difficult to disentangle via integrated light measures because of significant degeneracy with both age and metallicity (cf. Fig 37 of Worthey (1994)). Blue Horizontal branch morphology can increase the $H\beta$ index by as much as 0.75 \AA compared to clump (Lee et al. 2000). This shift gives the appearance that the globular clusters with blue horizontal branch morphologies are younger or more metal poor than they really are.

Schiavon et al. (2004) proposed that the ratio of $H\delta_f/H\beta$ is more sensitive to horizontal branch morphology than to age allowing us to break the degeneracy present between these two parameters. Graphs with $H\delta_f/H\beta$ versus iron indices have globular clusters with mostly blue horizontal branch morphologies that appear displaced relative to the locus occupied by the models, as shown in Fig. 9. Since in the Milky Way globular cluster system, the horizontal branch morphology changes from blue to red at around $[\text{Fe}/\text{H}] = -1$, there is some ambiguity with metallicity.

It is unlikely that a ratio of Balmer indices will be completely optimal for detecting an extended horizontal branch. Indeed, we know of no effort to optimize the integrated-light detection of horizontal branch types in the literature, so we provide a simple one in this work. The idea is to pick three indices, and force them to provide solutions for age, horizontal branch morphology, and metallicity; three equations in three unknowns. The models used as a base are the Worthey (1994) models because the horizontal branch can be forced to be clump, extended, or blue at any metallicity. Then an error assigned to each color, magnitude, or index yields a propagated error in age, morphology, or abundance.

The corners used for the linearization are ages 11 and 17 Gyr, $[\text{Fe}/\text{H}]$ of -1.8 and -0.6 ,

and morphologies either red clump or blue, where clump was assigned a numerical value of zero, and blue a numerical value of one. The models also come in an “extended” horizontal branch morphology that stretches from the red clump to $\log T_{eff} = 4.0$, but in this paper we only use those models for plots. The “blue” morphology has stars between $\log T_{eff} = 3.9$ and $\log T_{eff} = 4.1$. Errors were assigned to each index, and then used to do error propagation in the linear solutions, giving a goodness-of-fit for age, morphology, and metallicity.

An example of this is shown in Fig 10. For each trio of indices, the horizontal branch solution is on the y axis, and the metallicity solution is on the x axis. Model sequences for ages 8 and 17 Gyr are shown at 0.2-dex intervals from $[Fe/H] = -2.0$ to -0.2 , and the collection of Schiavon et al. (2004) indices are shown, symbols varying between $HBR < 0$ and $HBR > 0$, as in previous figures. In the figure the model sequences separate much more than the simpler Balmer index ratio plot. However, we caution that the models used are rather out of date, and better solutions might be found from more up to date isochrones.

3.3. Blue Stragglers

No provision for blue straggler stars are in the synthesis models. If such stars were present in the models, the Balmer line strengths would strengthen by several tenths of Ångstroms, in a sense to make the low-lying globular clusters lie even lower.

3.4. Emission Fill in

Filling in of the absorption lines due emission could change the depth of the lines present in the spectra. This change in depth will lower the Lick/IDS index value. Emission could be caused by many things, such as: Gas clouds in the line of sight, planetary nebula, supernova remnants, M dwarfs with active chromospheres, and AGB type stars.

For example, if we adopt a star formation region-like recombination spectrum for an optically thick nebula of 10^4 K and 10^4 electrons per cubic centimeter, Osterbrock (1989) gives the relative Balmer line intensities of $j\gamma/j\beta = 0.469$ and $j\delta/j\beta = 0.260$. For a given $H\beta$ index fill-in value, the equivalent widths of the $H\gamma$ and $H\delta$ indices can be predicted after correcting for (1) underlying continuum shape and (2) the widths of the indices themselves. Using values of $F_{c, \gamma}/F_{c, \beta} = 0.84$ and $F_{c, \delta}/F_{c, \beta} = 0.81$ for the relative continuum flux ratios, a one-Ångstrom fill-in of $H\beta$ propagates to fill-ins for the higher-order indices of $\Delta H\gamma_F = 0.76 \text{ \AA}$, $\Delta H\gamma_A = 0.37 \text{ \AA}$, $\Delta H\delta_F = 0.44 \text{ \AA}$, and $\Delta H\delta_A = 0.24 \text{ \AA}$.

Planetary nebulae can be seen, one by one, in Milky Way globular clusters, and only M5

has a planetary nebula, so they should be rare in M31 globular clusters as well. Supernova remnants are much more improbable. Gas clouds containing neutral sodium are known to exist along most lines of sight out of the galaxy (Bica & Alloin 1986) but there is no reason to expect ionized hydrogen to linger in the potential wells of globular clusters since the RMS velocity for a 10,000 K proton is $v_{\text{rms}} = (3kT/m)^{1/2} \sim 15 \text{ km s}^{-1}$ exceeds the escape velocity of all but the largest globular clusters. We thus discount these three explanations.

However, the stellar sources are less easy to discount. M dwarfs are known to have active chromospheres, although old ones get less active (West et al. 2008). In addition, Schiavon et al. (2005) observed a probable bright, red giant flaring in their spectra. This star is bright enough so that, by itself, it will alter the integrated Balmer line strengths. The character of these two sources is different, however, in that the numerous M dwarfs are spatially broad and should be nearly constant in Balmer emission output while the giants are spatially discrete, and should be highly time-variable. M dwarf light will still give a net Balmer emission signal because the M dwarfs are concentrated toward the center of the cluster, albeit less so than the more massive stars. In support of cool giants causing fill-in, the most metal-poor clusters do not have very cool giants. It is only at $[\text{Fe}/\text{H}] \approx -1$ and above that clusters begin to have long period variables and genuine M-type giants, and these are the clusters that show the anomalously low $\text{H}\beta$ strengths.

3.5. Models

Are the line depths of current sets of models too deep? The Worthey models agree quite well with more modern model sets, especially after rescaling the ages by subtracting 2 Gyr. If, however, all authors are making the same mistake and all Balmer line strengths should be dropped to a level to make the low-lying globular clusters fit along the old-age sequence, then there are some implications. First, even with correction for horizontal branch morphology, the metal-poor clusters will still look substantially younger. Second, the average elliptical galaxy will look young enough to raise eyebrows.

Despite this quandary, there may be one way to get the models to fit everything, or nearly everything, and that is to invoke fairly hefty abundance ratio systematics, especially with oxygen and helium, that could plausibly drift in opposite directions for metal-rich globular clusters versus elliptical galaxies. These effects would operate mostly on the isochrone temperatures and age scales, and not operate significantly on the integrated stellar spectra. However, in the absence of more direct observational evidence, this scheme is speculative.

4. Conclusion

Extracting information from the integrated light of stellar populations is not an easy process, since there are many complex factors affection the spectra. Decoupling the age-metallicity degeneracy by graphing Balmer line indices vs. metal feature indices has allowed us to learn much more about stellar populations, however the weakness of the observed $H\beta$ line relative to the models needs to be explained. This paper shows that altered abundance ratios, are unable to account for the observed weakness in the Balmer line strengths of globular clusters.

However, many other factors can potentially affect the Balmer line strengths that we must be aware of if we are to use them as age indicators. Horizontal branch morphology effects are hard to disentangle since they are also degenerate with age and metallicity. Also, we need to consider the simplifications that our models use, such as not including the presence of blue stragglers. Most importantly we must be aware that emission fill-in of the Balmer lines due to hydrogen recombination lines from either external nebulae or stellar activity in individual cluster star can effect the line depths. More investigation needs to be done to determine whether abundance ratios can cause isochrone temperature drifts.

The authors gratefully acknowledge support from National Science Foundation grants AST-0307487 and AST-0346347.

REFERENCES

- Beasley, M. A., Brodie, J. P., Strader, J., Forbes, D. A., Proctor, R. N., Barmby, P., & Huchra, J. P. 2005, *AJ*, 129, 1412
- Bica, E., & Alloin, D. 1986, *A&A*, 166, 83
- Busso, G., et al. 2007, *A&A*, 474, 105
- Coelho, P., Barbuy, B., Meléndez, J., Schiavon, R. P., & Castilho, B. V. 2005, *A&A*, 443, 735
- Dotter, A., Chaboyer, B., Ferguson, J. W., Lee, H.-c., Worthey, G., Jevremović, D., & Baron, E. 2007, *ApJ*, 666, 403
- Gratton, R., Sneden, C., & Carretta, E. 2004, *ARA&A*, 42, 385
- Greggio, L., & Renzini, A. 1990, *ApJ*, 364, 35
- Gunn, J. E., Stryker, L. L., & Tinsley, B. M. 1981, *ApJ*, 249, 48
- Harris, W. E. 1996, *AJ*, 112, 1487
- Lee, H.-c., Worthey, G., Dotter, A., Chaboyer, B., Jevremović, D., Baron, E., Briley, M. M., Ferguson, J. W., Coelho, P., & Trager, S. C. 2009, *ApJ*, 694, 902
- Lee, H.-c., Yoon, S. -J., & Lee, Y. -W. 2000, *AJ*, 120, 998
- O’Connell, R. W. 1986, in *Stellar Populations*, ed. C. A Norman, A. Renzini, & M. Tosi (Cambridge: Cambridge Univ. Press), 167
- Osterbrock, D. A. 1989, *Astrophysics of Gaseous Nebulae and Active Galactic Nuclei*, University Science Books, Mill Valley, CA
- Rabin, D., 1980, Ph.D. Thesis, California Institute of Technology
- Rabin, D., 1982 *ApJ*, 261, 85
- Sanches-Blazquez, P. et al. 2007, *VizieR Online Data Catalog*, 837, 10703
- Schiavon, R. P., Rose, J. A., Courteau, S., & MacArthur, L. A. 2004 *ApJ*, 608, 33
- Schiavon, R. P., Rose, J. A., Courteau, S., & MacArthur, L. A. 2005 *ApJS*, 160, 163
- Serven, J., Worthey, G., & Briley, M. M. 2005, *ApJ*, 627, 754

Trager, S. C., Worthey, G., Faber, S. M., Burstein, D., & Gonzalez, J. J. 1998, ApJS, 116, 1

Valdes, F., Gupta, R., Rose, J. A., Singh, H. P., & Bell, D. J. 2004, ApJS, 152, 251

West, A. A., Hawley, S. L., Bochanski, J. J., Covey, K. R., & Burgasser, A. J. 2008,
arXiv:0812.1223

Worthey, G. 1994, ApJS, 95, 107.

Worthey, G., Faber, S. M., Gonzalez, J. J., & Burnstein, D. 1994 ApJS, 94, 684

Worthey, G., & Ottaviani, D. L. 1997 ApJS, 111, 377

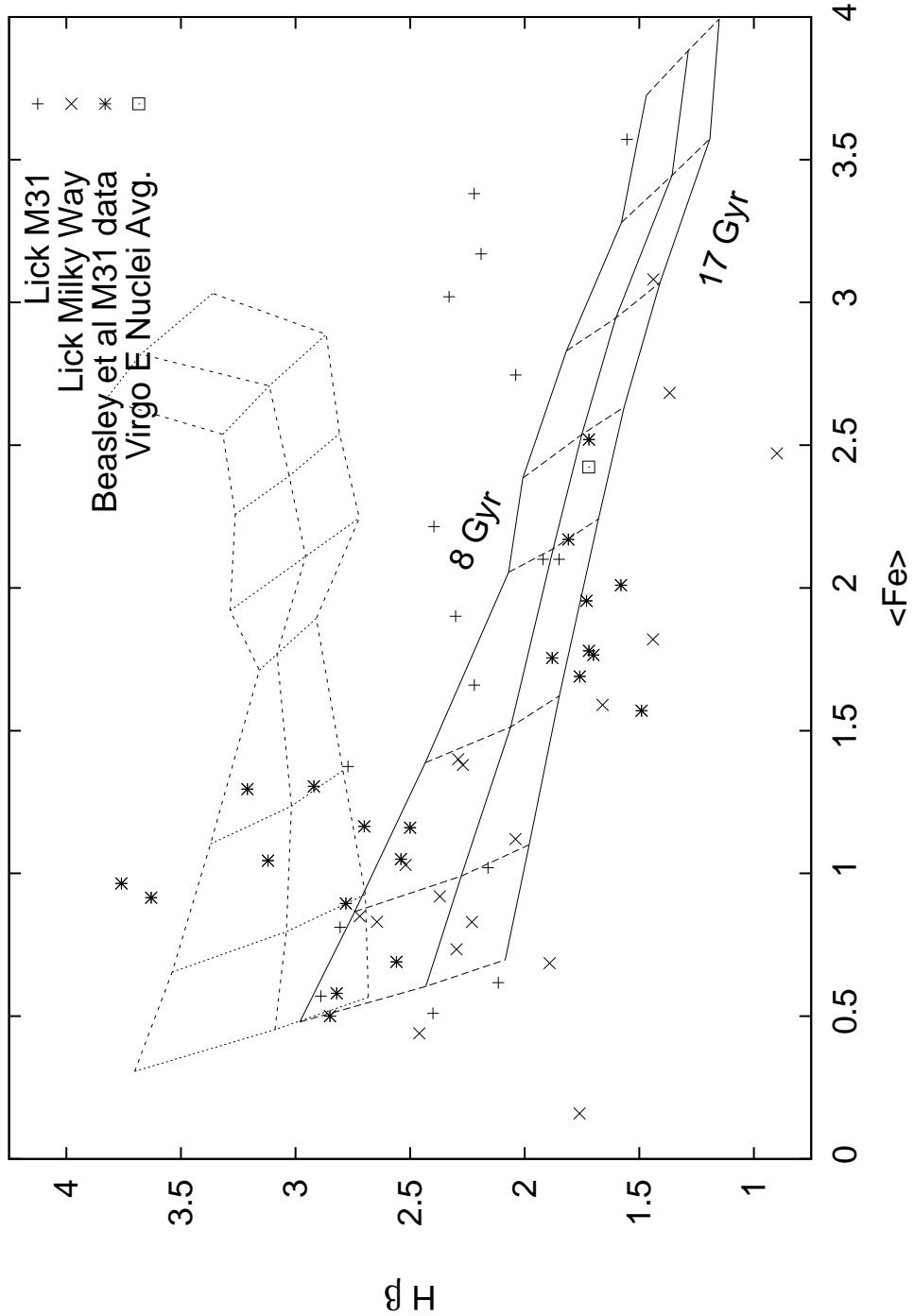


Fig. 1.— Literature data for Lick indices plotted for globular clusters in the Milky-Way and M31 (Trager et al. 1998; Beasley et al. 2005). Also plotted is an average of the Virgo elliptical galactic nuclei (J. Serven et al. 2009, in preparation). Two model grids (Worthey & Ottaviani 1997) are shown in this figure. The lower one has a forced red clump morphology for the horizontal branch, while the top grid has all hot horizontal branch stars. Even using different models, we still have the problem that some globular clusters are weaker in $H\beta$ than the reddest models, appearing much older than could be realistic.

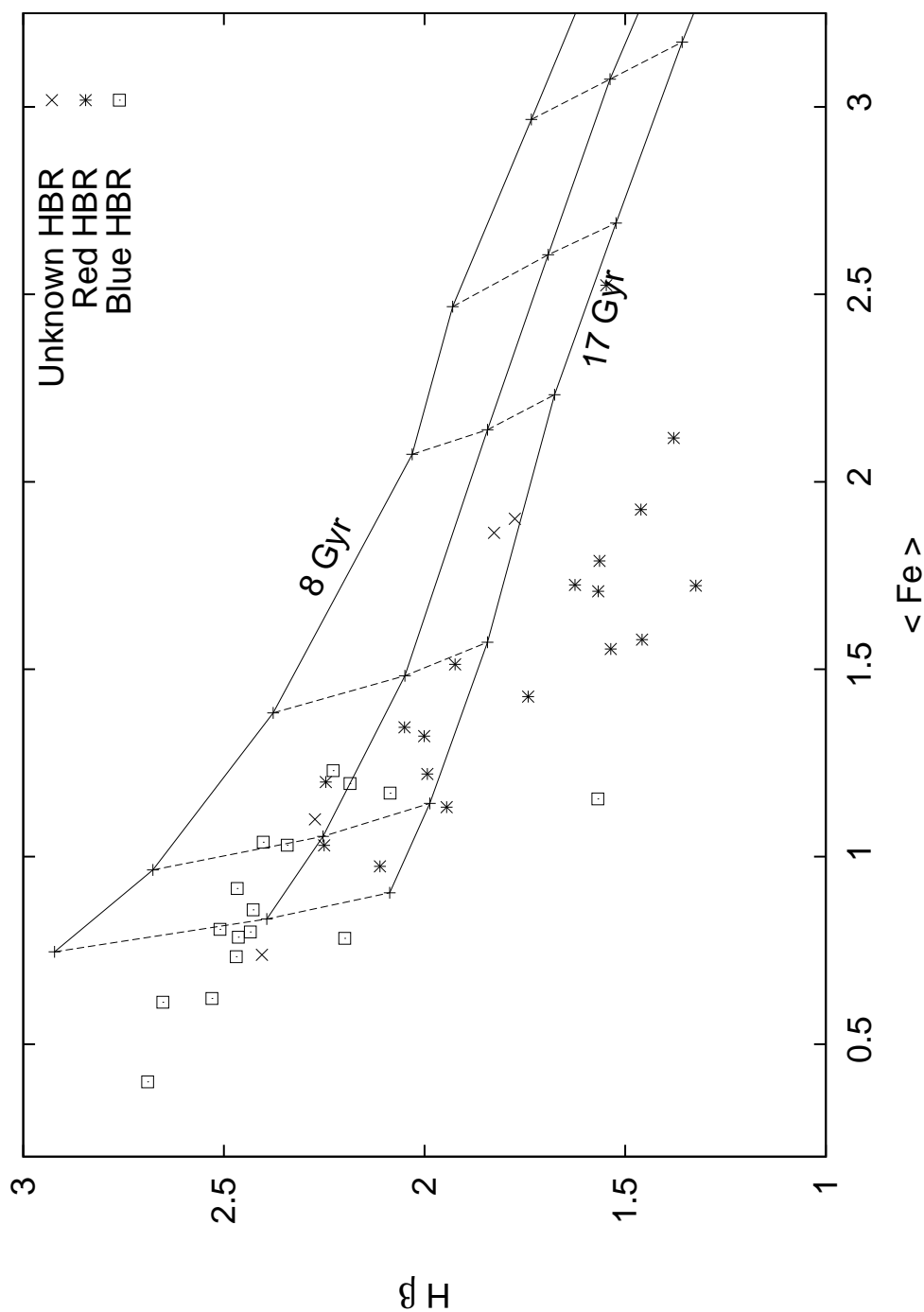


Fig. 2.— $H\beta$ and $\langle Fe \rangle$ indices for globular clusters (from Schiavon et al. 2005) and models. Red lines are models with ages: 8, 12, and 17 Gyrs from top to bottom. Blue lines are models at different metallicities. Globular Clusters are plotted on the same graph, divided into two groups. Red HBR, have $X_{HB} = (B - R)/(B + V + R)$ greater than zero, while Blue HBR type have X_{HB} less than zero. Both of the pair of Fe-strong blue X's (NGC 6388, NGC 6441) are known to have a partially blue horizontal branch (Busso et al. 2007).

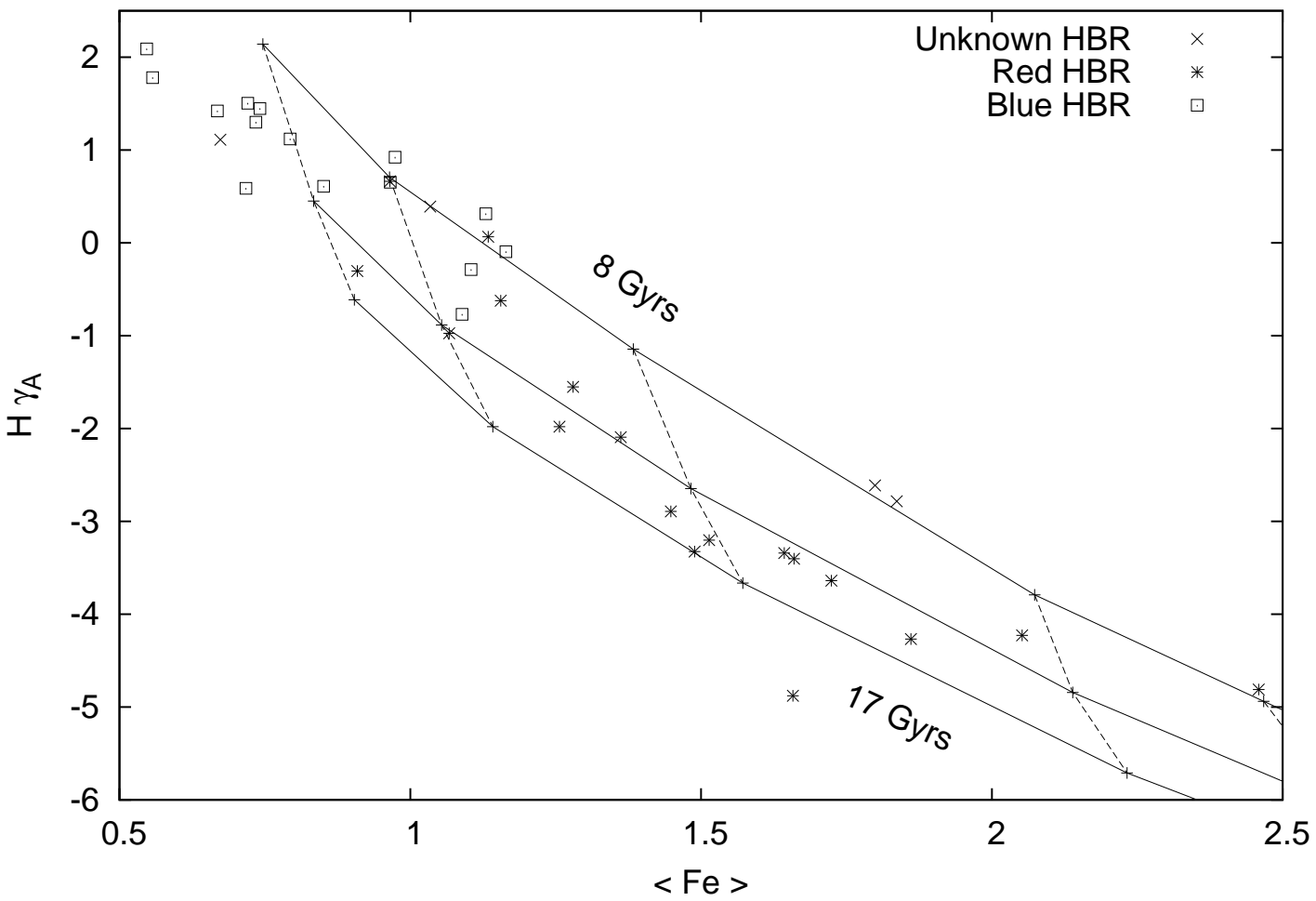


Fig. 3.— $H\gamma/H\beta$ versus $\langle \text{Fe} \rangle$ for globular clusters and models. Meanings of lines and symbols are the same as in Fig 2.

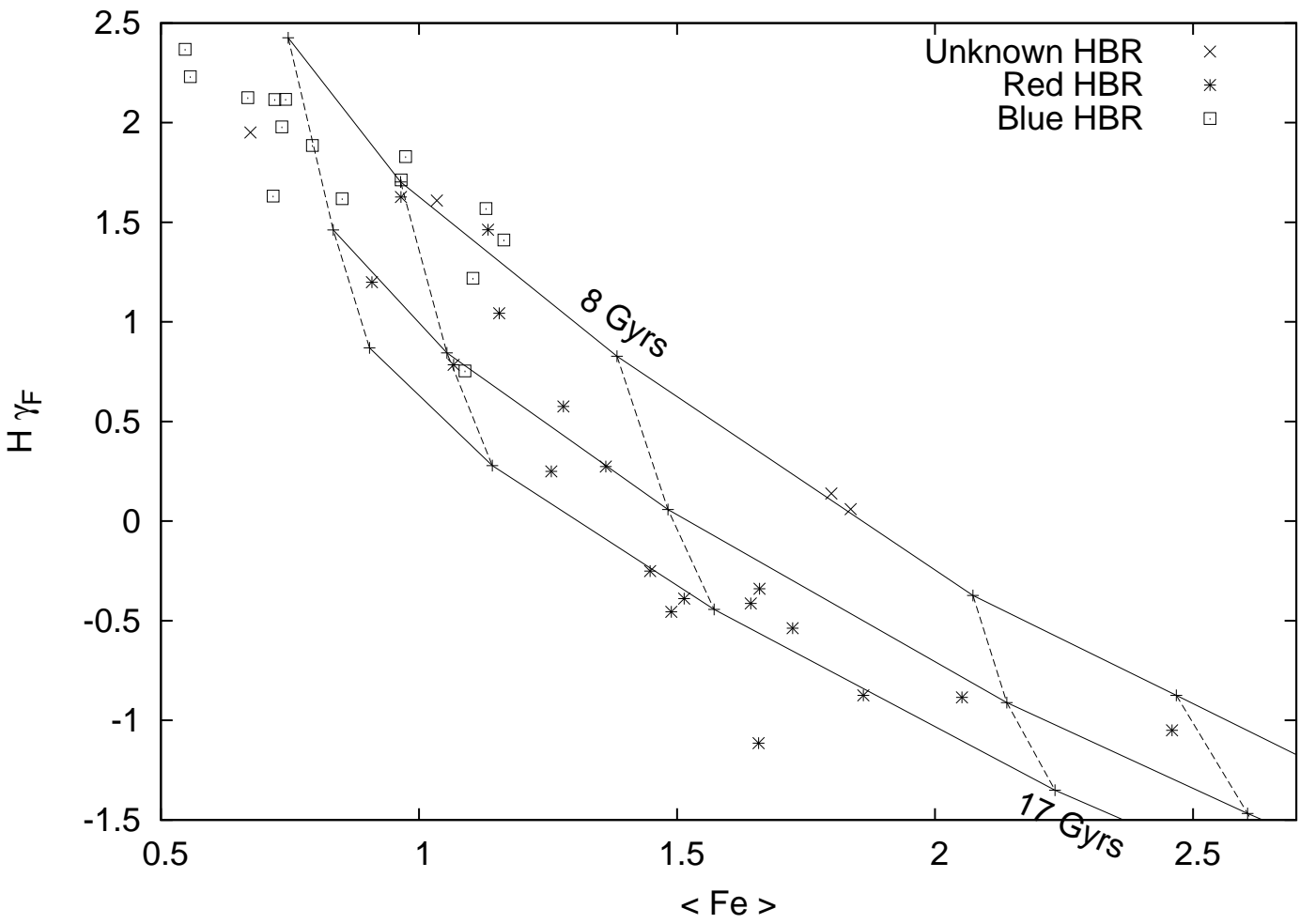


Fig. 4.— $\langle M_H \rangle$ versus $\langle Fe \rangle$ for globular clusters and models. Meanings of lines and symbols are the same as in Fig. 2.

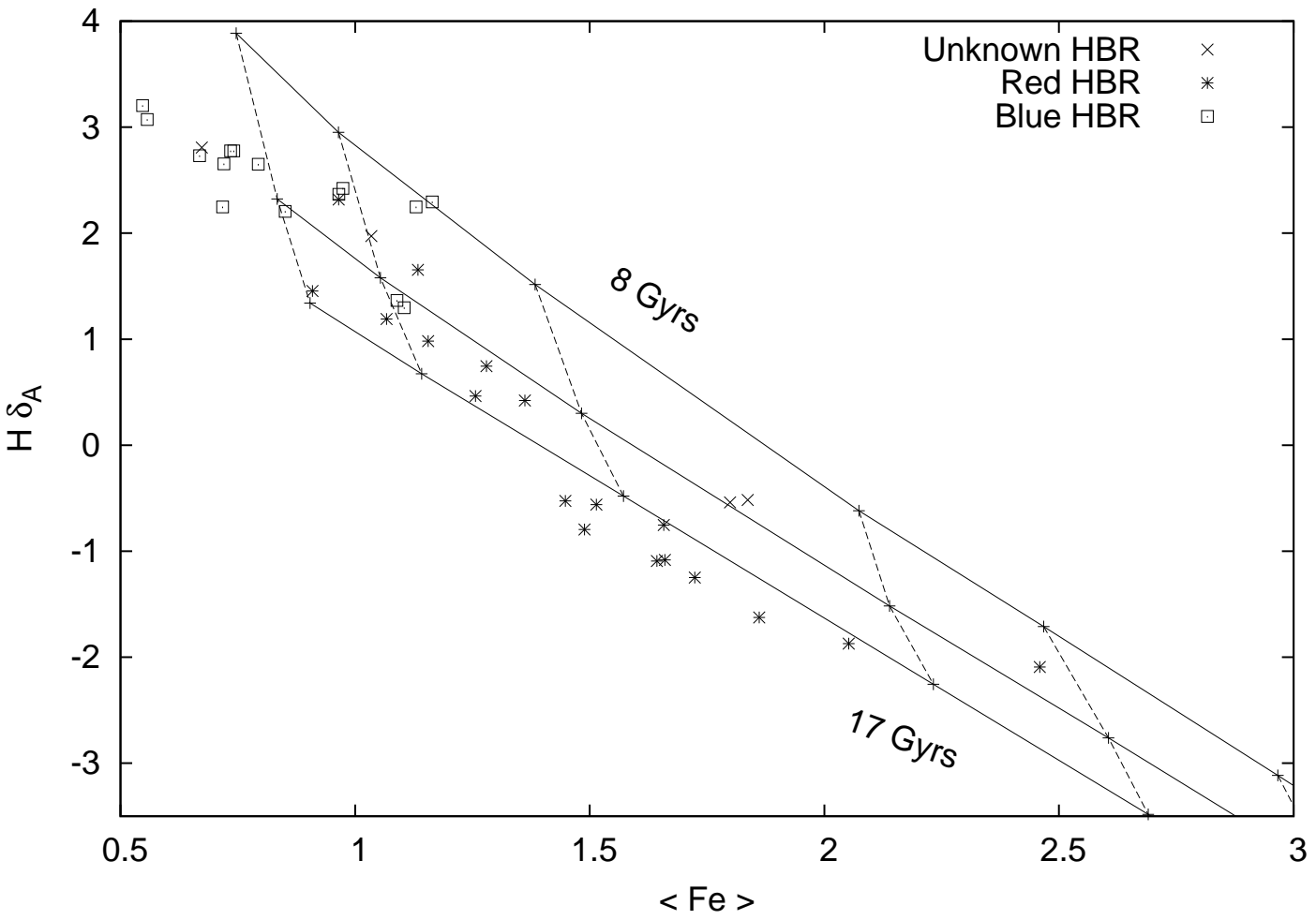


Fig. 5.— $\text{H}\delta_A$ verse $\langle \text{Fe} \rangle$ for globular clusters and models. The meanings of lines and symbols are the same as in Fig. 2.

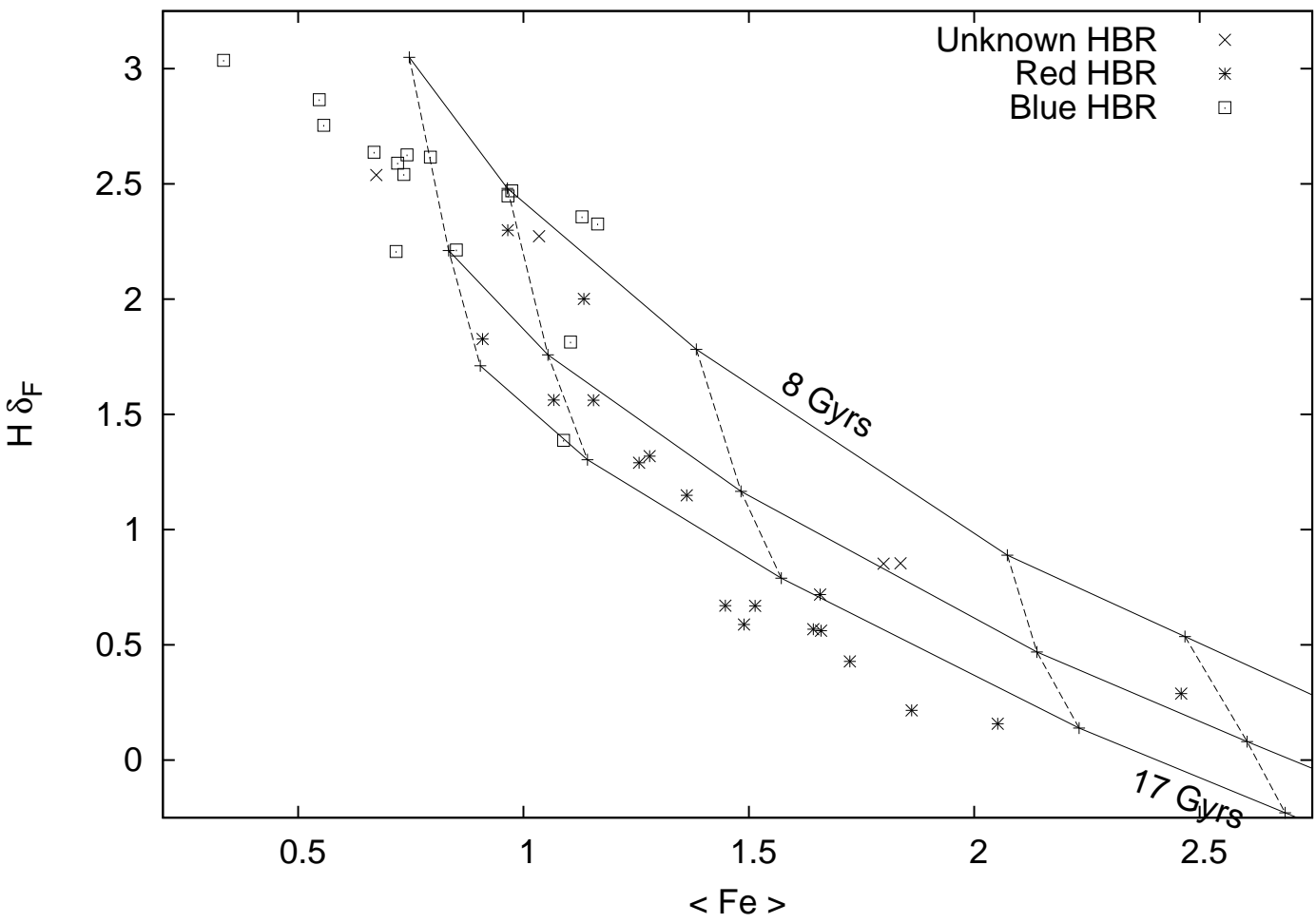


Fig. 6.— $H\delta_F$ versus $\langle \text{Fe} \rangle$ for globular clusters and models. The meanings of lines and symbols are the same as in Fig. 2.

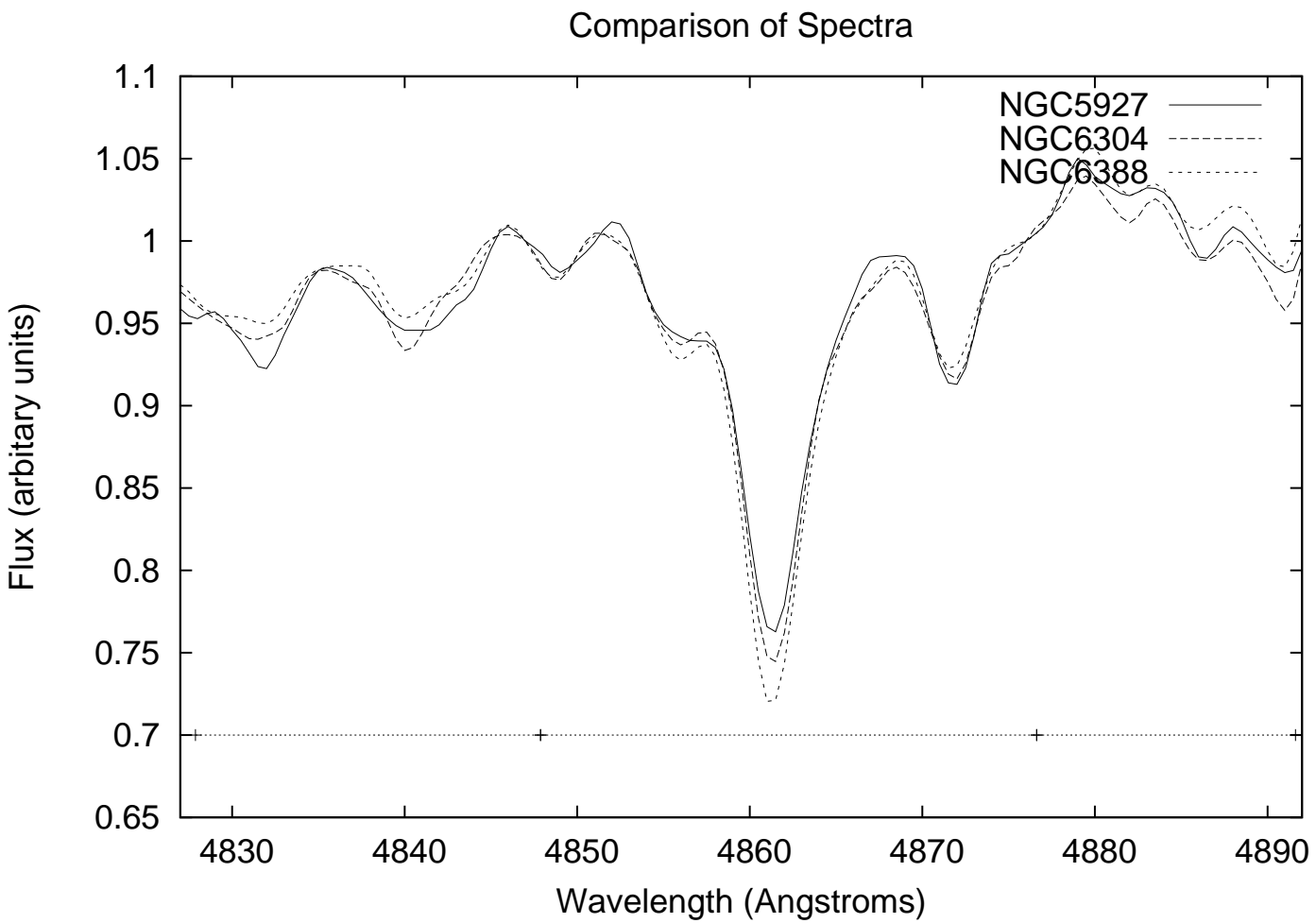


Fig. 7. — Comparison of the spectra of globular clusters at approximately the same metallicity. NGC 6388 appears on the age-metal grid while NGC 5927 and NGC 6304 are below the grid, and the stronger $H\beta$ feature is obvious.

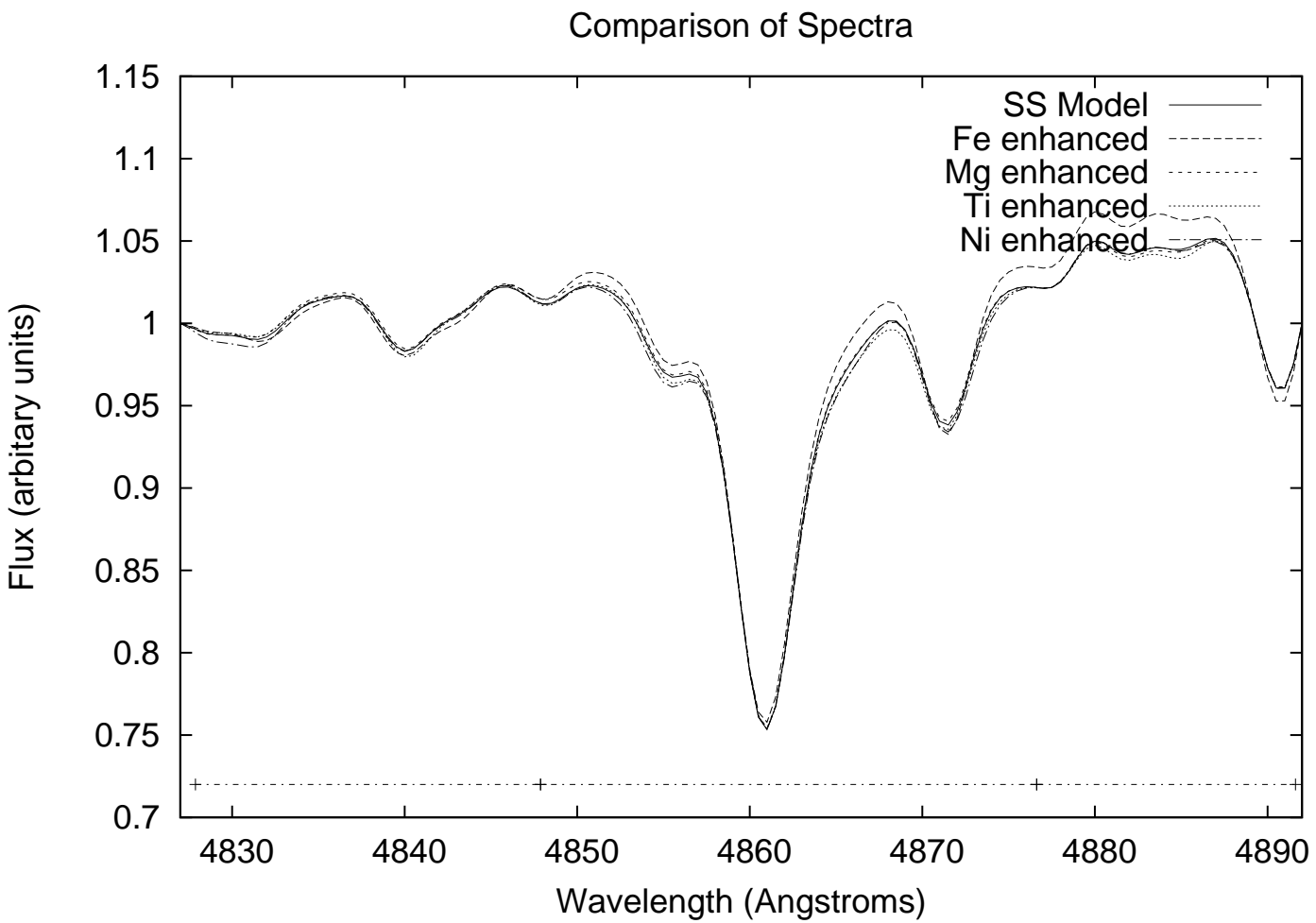


Fig. 8.— Comparison of model spectra near the H-Beta line, with various element enhancements. SS refers to scaled-solar, and the rest are enhanced by 0.3 dex, element by element, with total heavy element abundance held constant.

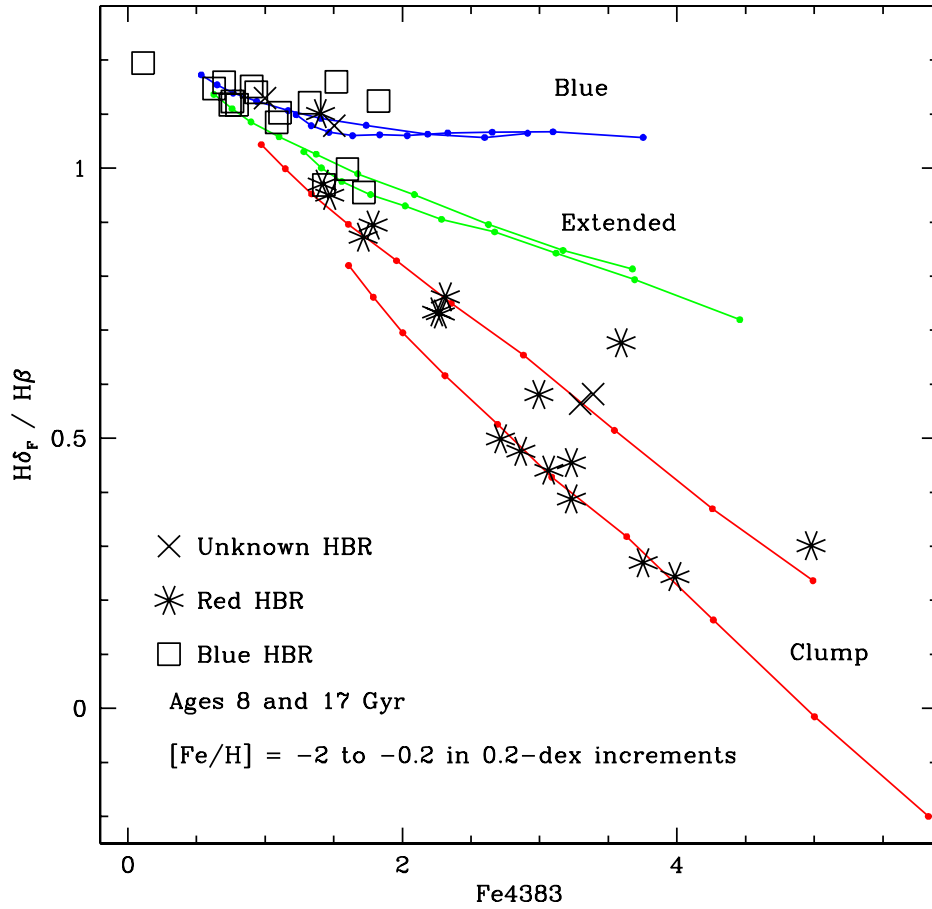


Fig. 9.— Balmer index ratio vs. Fe4383, a horizontal branch diagnostic diagram. Worthey (1994) Models for ages 8 and 17 Gyrs between $[\text{Fe}/\text{H}] -2$ and -0.2 are plotted in increments of 0.2 dex. The upper sequence has a horizontal branch morphology that is forced to be blue. The middle sequence represents a horizontal branch extended in temperature. The lower sequences represents a red clump morphology. Symbols for globular cluster data are as in previous figures.

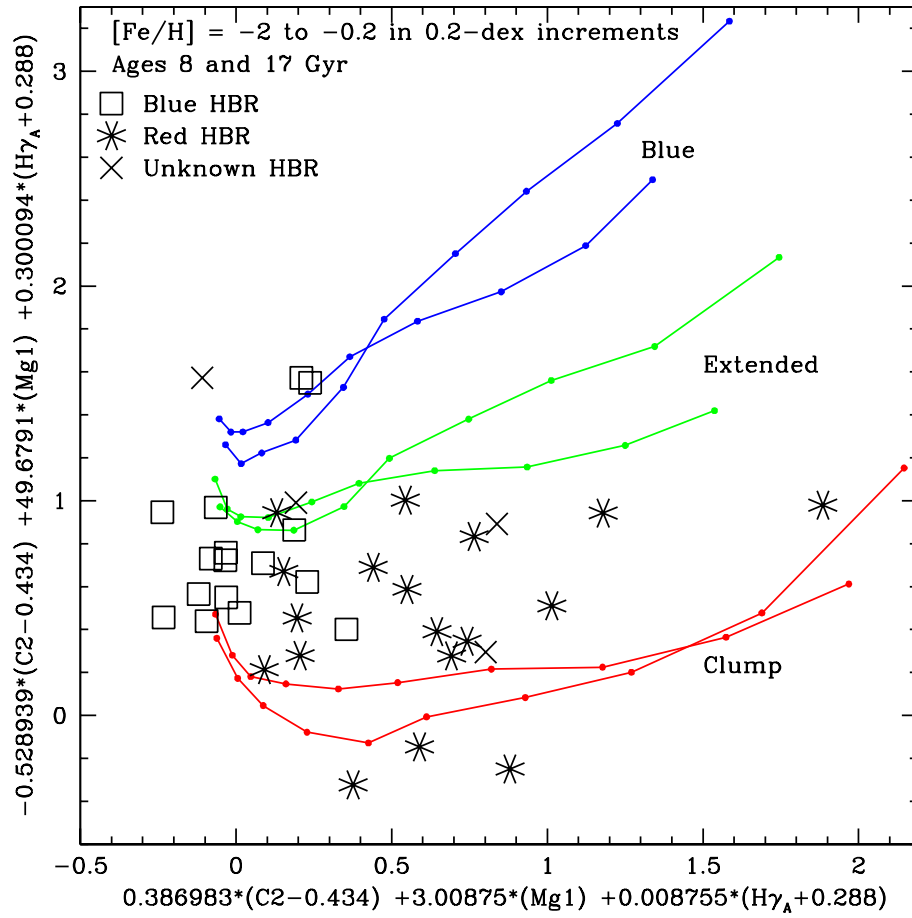


Fig. 10.— Example diagnostic index combination plot that attempts to separate horizontal branch morphology (y-axis) and metallicity (x-axis). Model sequences are as in Figure 9

Table 1: Spectral response of indices under various element enhancements

	H β	H δ_F	H γ_F	Mg $_b$	Fe5270	Fe5335
I_{OB}	1.522	0.613	-0.709	2.121	2.025	1.762
error	0.138	0.119	0.121	0.155	0.173	0.199
C	0.00	-0.16	-4.17	-0.19	0.16	0.06
N	0.00	-0.04	-0.03	-0.01	0.06	0.01
O	0.04	-0.11	0.76	0.12	-0.04	-0.01
Na	0.01	-0.01	0.07	-0.09	-0.03	-0.03
Mg	-0.29	0.16	1.12	4.83	-0.32	-0.26
Al	0.02	0.01	0.11	-0.06	-0.05	-0.05
Si	0.07	1.88	0.79	-0.32	-0.09	-0.07
S	0.00	0.00	0.01	0.00	0.00	0.00
K	0.00	0.00	0.01	0.00	-0.01	-0.01
Ca	-0.02	0.56	-0.21	0.06	0.06	0.03
Sc	-0.01	-0.03	-0.27	0.00	-0.14	0.03
Ti	0.28	-0.54	-0.10	0.01	0.28	0.14
V	-0.02	0.53	-0.02	-0.02	-0.05	0.01
Cr	-0.12	0.03	0.66	-0.86	0.10	0.39
Mn	-0.02	-0.41	-0.04	-0.09	0.09	0.04
Fe	-0.57	-2.62	-0.85	-0.79	1.88	1.54
Co	-0.02	-0.21	-0.01	0.00	0.13	0.16
Ni	0.61	-0.09	-0.11	0.00	0.06	0.00
Cu	0.00	0.00	0.00	-0.07	-0.01	0.00
Zn	0.00	0.00	0.00	0.00	0.00	0.00
Sr	0.00	-0.34	0.00	0.00	0.00	0.00
Ba	0.00	-0.06	0.00	0.00	0.00	0.00
Eu	0.00	-0.06	0.00	0.00	0.00	0.00
upX2	0.09	1.95	2.31	4.48	0.45	-0.21

Note. — Row 1 is the model index, row 2 is the uncertainty assuming a $S/N = 100$ at 5000 \AA , rows 3 through 25 list the change of index when the labeled element is enhanced by 0.3 dex, and the last row has all elements up by 0.3 dex.